Merging metrology with magnetic measurement: developing innovative and cost effective solutions for a flexible field mapper.
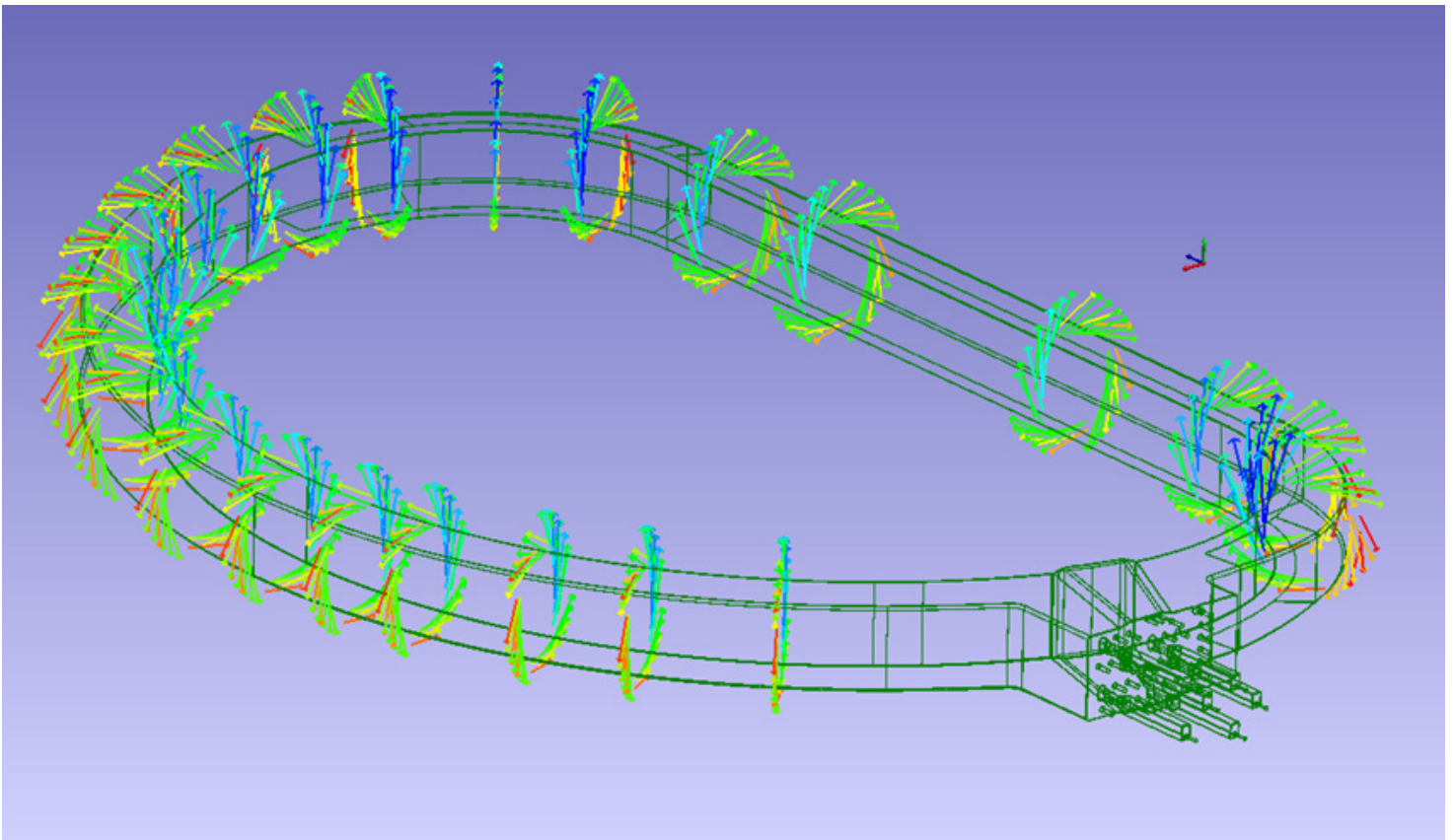
In magnet fabrication technology the effective magnetic field is the final indicator of the quality of the job.

Commercial solution are not flexible enough to cover all the needs of the workshop by using only one device.

This paper describes a flexible and innovative tool for the magnetic field mapping for the following case study: ITER Toroidal Field Coil Winding Pack WP magnetic flux density measurement.

# HIGH PRECISION MAGNETIC FLUX DENSITY MEASUREMENT

Alberto Barutti, Matteo Bargiacchi

Merging metrology with magnetic measurement: developing innovative and cost effective solutions.
When ASG started the engineering of the ITER contract and the development of the necessary fabrication technology it started as well to face a very challenging technological goal: how to obtain very large component with high accuracies. Fusion for Energy (F4E), our customer, asked for the definition of some indicators for the as-built performances,
after the coil manufacturing, to check that the product quality fulfils the requirements and to allow the integration inside the reactor of the components supplied by ASG with the others produced by other firms.

The most important key indicators in the definition of our coils as-built performances were identified to be:
— the as built dimensions
— the insulation system performances
— the room temperature magnetic field fingerprint. This is an indicator that allows to understand the quality of the internal geometry of the coils without accessing to the internal part of the coil.

Once the WP is completed it is not possible to access the internal components; the final assembly on the reactor must be driven by using a combination of the results of the test campaign during fabrication and after completion.

Cold tests campaign, that could allow to reach a field big enough to make easy measurements with large accuracies, is too expensive and not included in our scope of supply. Therefore, we decided to design a tool in order to guarantee enough accuracy to make the reconstruction of the magnetic field around the coil possible, by solving an inverse problem, with a very low field. This was useful also because at room temperature it's not possible to feed the coils with high current to avoid heating and large component deformations.

A first step was the Design of Experiment, whose results were the main parameters for the test design:
— Requirements of the workshop area.
— Huge number of points to be measured.
— Position and field measurements accuracy.
— Maximum current on the coil (i.e. maximum field available) in order to avoid thermal deformations.

The tool should have been robust, industrial, within time and budget: no ready commercial solution was available.

— **Goal**: obtaining a map of the magnetic field around the coil at standard temperature
— **Delighter**: speed and flexibility of the measurement system
— **To solve**:
  →  No commercial solution available.
  →  Required accuracy is close to the best available technology.
  →  We are an industry, not a laboratory.
  →  Very low magnetic field: approximately 150 G (15mT).
      As a comparison, the earth magnetic field is approximately
      1000 times smaller (0.5G = 50μT) and the peak field
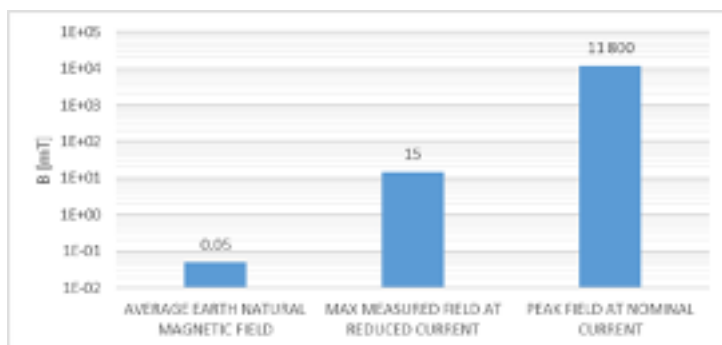      of the magnet is 1000 times bigger (118 000 G = 11.8 T).



**Figure 1**. Magnetic field ranges in logarithmic scale.

Only after a long scouting some custom solutions was found, but they seemed too difficult to be developed in a timely manner, not robust enough and with poor flexibility. In the scouting process we understood that a flexible solution should be preferred, both for the scope of the project and for future transfer to other applications.

A flexible field mapper, in fact, is needed for environmental field mapping, including the fringe field on the installations, the fringe MRI field mapping and many other uses. In particular, such technology is useful where it is necessary to sample a big number of measured points in a short time, with no predetermined location in space but with a precise knowledge of their position (it will be shown that it is possible to get points with a precise positioning).
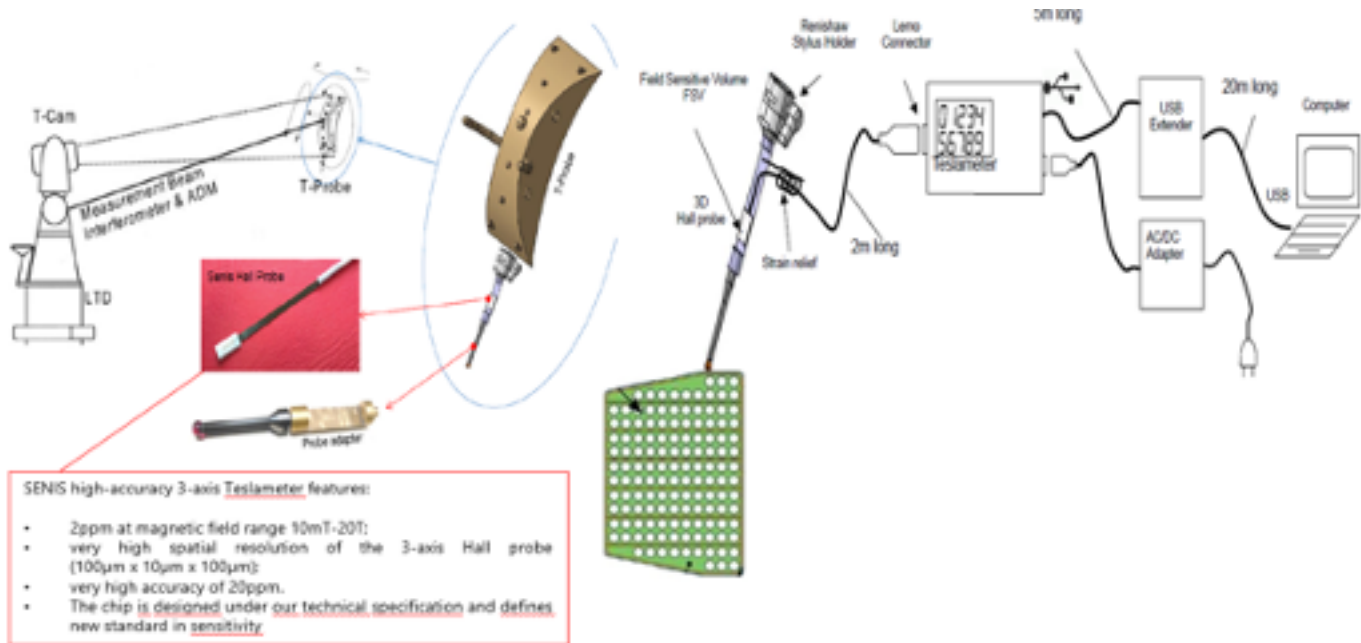
All these reasons convinced us to turn to an internal solution, by adapting the technology and know-how already in our possession.

So, we started to implement our solution, based on the merging of two supposedly distant worlds, metrology and magnetic measurements, which turned out to be an innovative measurement system based on a laser tracker and a Hall probe.

The main advantages of this configuration are:

— The possibility to share the same reference system between metrologic and magnetic measurements (and correlating results).
— The flexibility to measure objects with virtually all shapes and dimensions (no theoretical limit to dimension).
— It is possible to map a large volume of space obtaining the three components of the magnetic field and the position of the probe immediately with one measurement.
— Thanks to the innovative design of the hall probe (with a very small sensible volume) it is possible to operate in highly inhomogeneous magnetic fields without significant loss of information.
For a smarter use of this system, we developed a software plugin that allows to measure the magnetic field directly through the GUI (Graphic User Interface) of the commercial metrological software that we have adopted for the laser tracker management, making it easier to use the tooling and the generation of the output.

SENIS high-accuracy 3-axis Teslameter features:

- 2ppm at magnetic field range 10mT-20T;
- very high spatial resolution of the 3-axis Hall probe (100μm x 10μm x 100μm);
- very high accuracy of 20ppm.
- The chip is designed under our technical specification and defines new standard in sensitivity.

## 1. Introduction and scope of the measurement campaign within the ITER project

[1] https://www.iter.org/mach/magnets

Regarding the ITER TF project, each of the 18 Toroidal Field Coils Winding Packs (TFC-WPs) is composed of 134 turns made of niobium-tin ($Nb_3Sn$), generating a peak field of 11.8T and storing 41GJ[1]. Fabrication and assembly tolerances might generate sensible deviations from the expected nominal field generated inside the Tokamak.

The magnetic Flux Density Field $\vec{B}$ generated by the TF coil is therefore characterized through the definition of the Current Center Line (CCL) of each TFC-WP. The CCL is defined as the *single turn* that best approximates the field generated by the complete winding of each single TFC-WP, i.e. the solution of the inverse problem that minimizes the difference between the measured and nominal values of the magnetic field $\| B_M - B_N \|$, and represents the fingerprint of each coil. Current specifications for the ITER project require the reconstruction of the 3D position of the CCL for each TFC-WP, for the purpose of using these data during the final alignment of the coil inside the Tokamak. In order to achieve such a goal, it is essential to measure the field produced by the TFC-WP, at room temperature, with a tight accuracy.

## 2. The instrumentation concept, calibration and uncertainty essentials

A fully integrated 3-axis Type C hall probe[2] has been designed and realized in order to map the 3D field generated by the TFC-WP. Hall Effect is a well-known principle widely used for a broad range of applications, from proximity sensors in their simplest forms, to magnetometers. Hall Effects is based on the Lorentz force that electric charge carriers experience while travelling in a conductor immersed in a transverse magnetic field $B$. The displacement of the charges within the sensor generates an electric field mutually perpendicular to the current I and B. The hall probe sensible volume HSV measures 0.1 × 0.1 × 0.1 mm: it is embedded into an outer volume of about 8 x 4 x 0.9mm3 and mounted on the stylus of a Leica T-probe[3] as shown in Figure 3. The Leica T-Probe is a 6 Degrees of Freedom PCM device (Portable Coordinate Measurement) based on the combination of photogrammetry and an Absolute Laser Interferometer (AIFM). A T-probe simultaneously measures the position and the orientation of the device. Such a feature is essential to characterize the HSV with respect to the absolute reference frame of the object under measure.

[2] https://www.senis.ch/magnetometer/hall-probes

[3] https://www.hexagonmi.com/it-IT/products/laser-tracker-systems/leica-probing-solutions/leica-tprobe
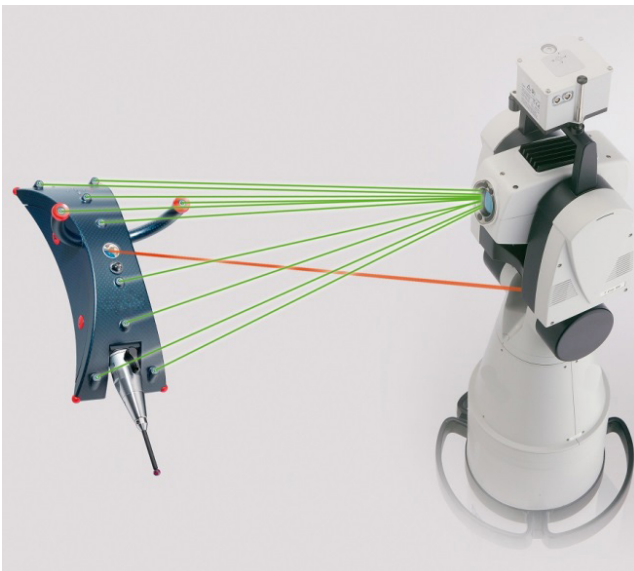


**Figure 2**. Leica Laser Tracker 6 DOF system (T-Probe). The position of the reflector is measured via the AIFM (red beam). The orientation of the device is measured via the T-Cam and a set of LEDs embedded on the surface of the target device (green beams).

Figure 3. ASG integration of a SENIS Type C Hall Probe inside the stylus of a Leica T-Probe. The white cable connected to the electronics supplies the DC current to the sensor and measures the DC voltage generated by the Lorentz force. A reference frame is defined centered on the T-Probe.



Figure 4. A picture shot during the R&D activities in 2016 on a WP, before its ground insulation.

This device concept requires a careful calibration activity. In practice, a set of matrix transformations is necessary to retrieve the real magnetic field from the raw magnetic field measured by the Teslameter and the 6 DOF measured by the T-Probe. This was the main activity carried out during the last months of 2016 and the first half of 2017 up to the first successful measure of the magnetic field generated by a WP, performed in June 2017. The accuracy with which the transformations matrices are calculated greatly influences the accuracy of the final measure. The calibration activity determines the final uncertainty of the measure and is the core of the present work.

The absolute field defined with respect to the absolute reference frame TGCS (Tokamak General Coordinate System, see Figure 12, later in this paper) of the object under analysis is $\vec{B}_{TGCS}$. This is the final output, starting from the raw field vector $\vec{B}_H$ that the operator can to read on the screen of the Teslameter. Anyway, the Teslameter does not know the orientation of the 3 axis of the HSV with respect to the absolute reference frame. Two transformation matrices $\underline{R}$ and $\underline{C}$ must be applied to the vector $\vec{B}_H$. Matrix $\underline{R}$ is a pure roto-translation (orthogonal matrix) coming from the Euler angles of the T-probe stylus $R_x$, $R_y$ and $R_z$ and absolute position $\vec{r}$. It requires no additional calibration and varies in each measure, according to the orientation of the T-probe with respect to the absolute reference frame. Matrix $\underline{C}$, on the other hand, is a non-orthogonal matrix resulting from calculation, and constant for all the measures.

The calibration of the system is embedded in matrix $\underline{C}$. The raw field vector $\vec{B}_H$ is roto-translated according to the Leica angles $R_x$, $R_y$ and $R_z$ and absolute coordinates vector $\vec{r}$ to obtain the field referred to the absolute system $\vec{B}_{TGCS}$. The expression is:

$$\vec{B}_{TGCS} = \underline{R} \cdot \underline{C} \cdot \vec{B}_H = \underline{R} \cdot \vec{B}_{T\text{-}Probe}$$

It is straightforward to understand that the so called calibration matrix $\underline{C}$ is a function of the orientation of the hall axes with respect to the T-probe axes. Its definition is:

$$\underline{C}^{-1} = \begin{bmatrix} \vec{x}_H^T \\ \vec{y}_H^T \\ \vec{z}_H^T \end{bmatrix}$$

Each line of matrix $\underline{C}$ is the transposed vector representation of each hall axis in the reference frame of the T-probe (see Figure 3).
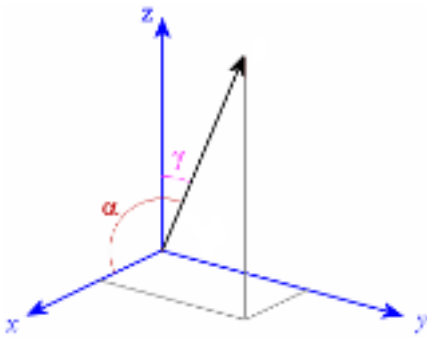


**Figure 5**. Vector representation of a single Hall probe axis inside the xyz T-probe reference frame (r = 1). Frame in figure is the same shown in Figure 3.

Actually, the chain of measure requires a careful calibration at different level to minimize the uncertainty related to the measure. Low level calibration and temperature corrections is provided directly by SENIS, the probe supplier, via firmware integration. This will be included in the uncertainty model but is not the object of this paper or of additional evaluations. We will see that its contribution to the final uncertainty will be automatically included during the calibration process. Geometrical calibration, synthetized in the constant calibration matrix $\underline{C}$, is essential to compensate for the following assembling imperfections:

1. Non orthogonality of the hall probe's axes $\mathcal{H}\mathbf{no}$
2. Misalignment of the hall probe's orthogonalized axes $\mathcal{H}\mathbf{o}$ with respect to the orthogonal T-Probe axes $T$

| Variable | Symbol | Correction applied | Application level |
| --- | --- | --- | --- |
| Voltage output | $\vec{U}_{RAW}$ | — | Firmware |
| Corrected voltage output | $\vec{U}_T = \vec{U}_T(\vec{U}_{RAW})$ | Temperature compensation | |
| Raw field | $\vec{B}_H = \vec{B}_H(\vec{U}_T)$ | Standard calibration curve from -40mT to 40mT per each component | |
| Orthogonalized Field aligned to T-Probe relative reference frame | $\vec{B}_{T\text{-}Probe} = \underline{C} \cdot \vec{B}_H$ | Sensitivity evaluation with respect to 3 orthogonal axes + Orthogonal rotation with respect to relative (T-probe) axes | Constant calibration matrix applied in the software $\underline{C}$ |
| Field aligned to absolute reference frame | $\vec{B}_{TGCS} = \underline{R} \cdot \vec{B}_{T\text{-}Probe}$ | Roto-translation | Variable transformation matrix $\underline{R}$ applied at each measured point |

Calibration and uncertainty evaluation were at first performed in collaboration with the Italian National Institute for Metrologic Research (INRIM[4]) in 2017. INRIM supplied a calibrated Helmholtz Coil[5] that was used to produce a steady and uniform reference field in the measurement range (see Figure 6). The reference field is aligned to the X axis of the HH coil and its homogeneity ΔH / H is smaller than 1e-4 in a sphere of 10 mm radius. This feature allows to place the HSV inside a homogeneity volume that is big enough to assume that the field measured is always the same in the absolute reference frame of the HH coil aligned to the Laser Tracker.

[4] https://www.inrim.it/

[5] F. Fiorillo, G.F. Durin, L. Rocchino, A reference system for the measurement of low-strength magnetic flux density, Journal of Magnetism and Magnetic Materials, Volume 304, Issue 2, 2006.

Essentially, the HH Coil from INRIM was used to calculate the calibration matrix $\underline{C}$. The hypothesis is that the reference field $\vec{B}_{REF}$ inside the homogeneity volume is constant regardless the position and orientation $\underline{R}_i$ of the sensible volume. The raw data from the 3 axis of the sensor $\vec{B}_{Hi}$ and the matrix $\underline{R}$ are registered and an GRG optimization loop is deployed to calculate the best coefficient of the calibration matrix $\underline{C}$.
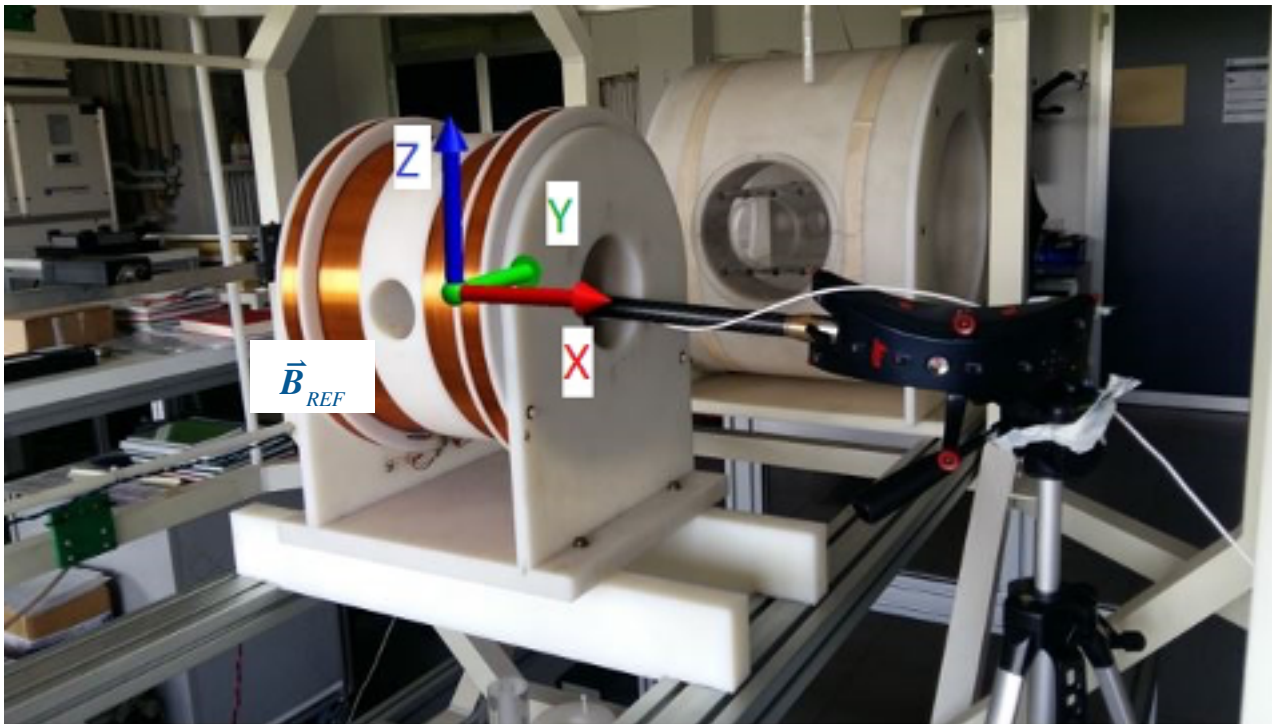


**Figure 6**. Calibration and uncertainty evaluation using a certified HH Coil @ INRIM.

The target function of the optimization is $J(\underline{C})$, defined as follows:

$$J\,(\underline{C},\ \vec{B}_{REF}) = \sum_i \| \vec{B}_{REF} - \underline{R}_i \cdot \underline{C} \cdot \vec{B}_{Hi} \|$$

The optimization parameters are the components of matrix $\underline{C}$ and the 2 Euler angles of the reference field $\beta_x$, $\beta_z$, that, in principle, are not known a-priori with enough precision.

The geometrical centre of the HH coil is detected probing the surface of the coils. High accuracy is not necessary, as the homogeneity volume is big enough to allow some errors in the evaluation of its centre.

Anyway, the optimization process produces an orientation of the reference field $\vec{B}_{REF}$ that differs from the geometrical approximation by 14.7 *mrad* and $\beta_z$ and 0.5 *mrad* for $\beta_z$ only. Nevertheless, the magnitude of these angles does not influence in any way the calibration procedure, as the reference field is fixed and uniform regardless of its orientation. Anyway, they give a good grasp of the quality of the geometrical characterization of the HH coil.

A campaign of 90 different measurements, with different combinations of current applied to the coils and orientation of the probe, was performed. The set of positions was chosen in order to have the minimum condition number for the system to be solved, i.e. to have enough orientation to maximize the sensitivity for each axis of the hall probe.

Mathematically speaking it is an over-constrained non-linear system of 90 equations with 8 unknowns to be solved via an iterative approach. The distribution of the relative error with respect to the reference field

$$\varepsilon\% = \frac{\| \vec{B}_{REF} - \vec{B}_{MEASi} \|}{\vec{B}_{REF}}\ \%$$  is shown in Figure 7.

The average is found to be 0.13% with a standard deviation of 0.05%. These numbers include also the uncertainty on $\vec{B}_{Hi}$ and on $\underline{R}_i$ produced by the Teslameter and by the Laser Tracker respectively.
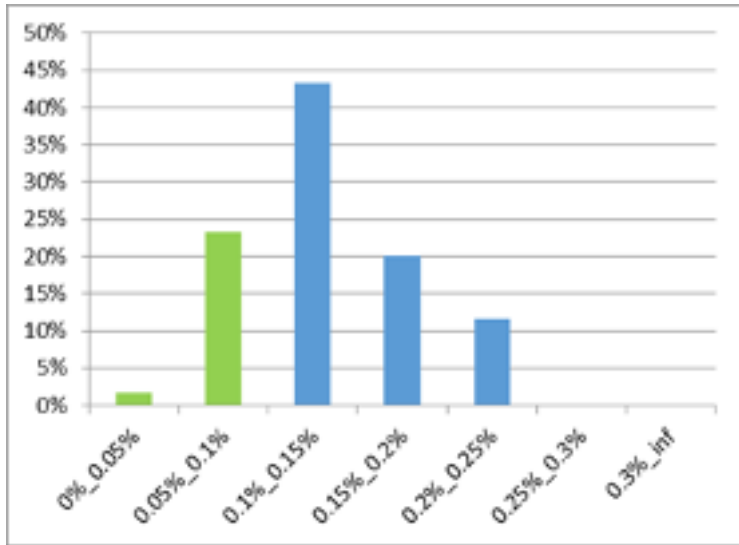
**Figure 7**. Distribution of relative error ε% of the measures after application of the calibration matrix.

A model for the uncertainty is calculated as follows:

$$U_{B_{Ai}} \approx \sqrt{(U_{B_{Hi}})^2 + (B_{Hi}\, U_{C_{ij}})^2}$$

Where $U_i$ is the uncertainty on the *i-th* quantity.
The final uncertainty of the complete system is evaluated to be

$U_{C_{ij}} \approx 0.23\%$ @2σ for any measure performed in the applicable range

of the campaign. $U_{B_{Hi}} = 7\mu T$.

A similar HH coil, characterized by 4 fiducials, was lately developed in order to perform in-house calibration in any moment.

**Figure 8**. A similar HH coil developed to perform the calibration procedure in house.

| | |
|---|---|
| Magnetic field range | 1mT - 20mT; Short time 50mT |
| Maximal current (for 20mT) | 1.4A |
| Helmholtz Coil constant k = B/I [mT/ A] | 14.353 mT/A |
| Non-linearity error in the applicable range (after 30') | 1e-5 |
| ΔH/H in 20mm sphere | < 4e-4 |
| ΔH/H in 2mm sphere | < 4e-5 |
| Resistance (series connected coils) | 63 Ω |
| Turns | 2 x 2200 x |
| Wire diameter | Ø1mm |
| Max power | 125W |

## 3. Examples of measured magnetic field

A tool is developed in .net Framework to coordinate the measurements of the Laser Tracker and the Teslameter all within a SpatialAnalyzer® (SA) environment. The software can instantly visualize the vector of the magnetic flux density inside the 3D environment of SA aligned to the CAD model of the object under inspection.

The tool was initially implemented to be flexible enough to measure a vector $\vec{B}$ in any visible and accessible position. For the present purpose some additional features were developed to streamline the process of acquisition and facilitate the sequence of actions to be performed by the operator (e.g. switch on/off the power supply of 200A DC or measure control points).

Depending on the measurements accuracy, the procedure might need a physical tool to precisely move the T-probe and keep it in a steady position for each single acquisition. If minor accuracy is acceptable, the T-probe could be moved by hand and the acquisition process might be significantly faster.
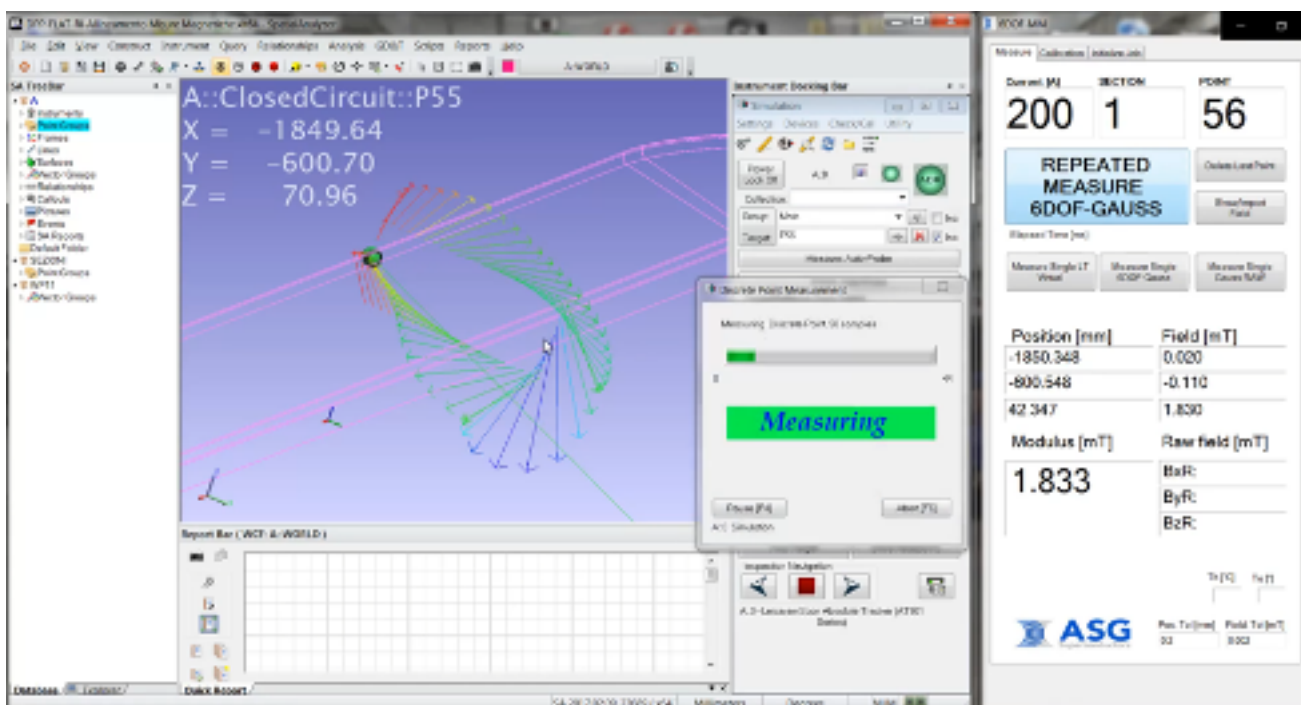


**Figure 9**. Snapshot of the GUI to control the 6DOF-MM device within SA.

A preliminary test was performed on the Double Pancake Prototype (DPP) coil. The line integral of the magnetic field around a closed loop was measured ($\Gamma(\vec{B})$) and calculated from theory ($\Gamma_{CALC}$). The relative difference was found to be only 0.14% despite the coarse grid used for the numerical approximation of the integral.

$$\Gamma(\vec{B}):=\oint \vec{B}\cdot d\vec{l}=\oint \vec{B}\cdot d\vec{l} \approx \frac{1}{2}\sum_i (\vec{B}_i + \vec{B}_{i+1})\cdot(\vec{r}_{i+1} - \vec{r}_i) = -4530.2 \; mT\cdot mm$$

$$\Gamma_{CALC} = \mu_0 \sum_i I_i = -4\pi \cdot 10^{-7}\cdot 12 \cdot 300 \; T\cdot m = -4523.9 \; mT\cdot mm$$

$$\varepsilon_\Gamma = \frac{\Gamma(\vec{B}) - \Gamma_{CALC}}{\Gamma_{CALC}}\% = 0.14\%$$
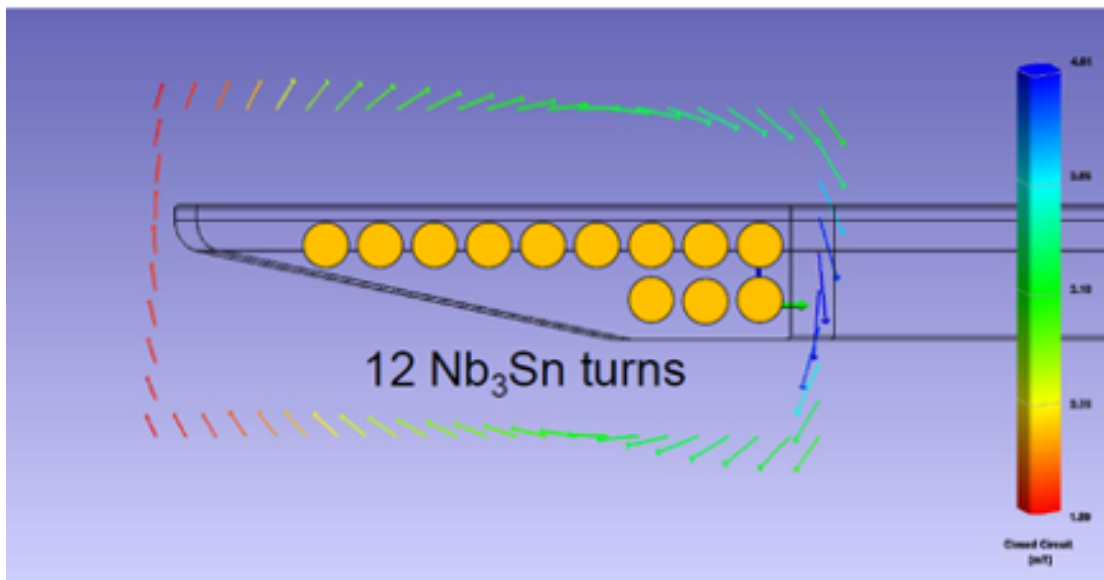


**Figure 10**. Line integral measure around a section of Double Pancake Prototype (DPP).

Measures on the WPs cannot be performed at nominal current of 68kA due to physical constraints. Therefore, a steady DC current of 200A is applied to the winding. The higher the current, the lower the noise to signal ratio. So, in principle, the current should be maximized. Pre-existent studies and practical tests had shown that, to avoid significant deformations due to thermal expansion, it is necessary to keep an unsteady current throughout the duration of the whole survey. The complete set of measurements could take up to 40 non-consecutive hours, therefore waiting for the thermal stabilization of the system is not worth the effort. For this reason, the current is switched on and off at each measuring section in order to minimize the thermal drift and avoid temperature compensations. Current stabilization is long enough to neglect any contribution from eddy currents.

All the ten Toroidal Field Winding Packs manufactured in ASG were measured with the described technique. Some snapshots of the WPs measured in 2017 are shown in the following pictures.
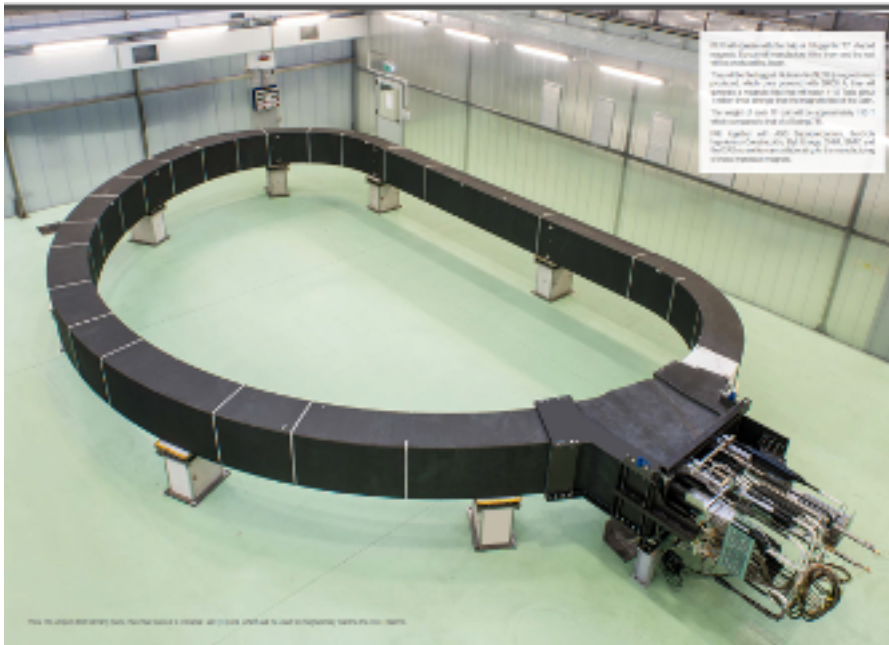


**Figure 11**. View of a WP inside the dedicated a-magnetic clean area at ASG premises (La Spezia). White tape visible on the coated surface was used to visualize the location of the sections to be measured and simplify the preliminary alignment of the device.
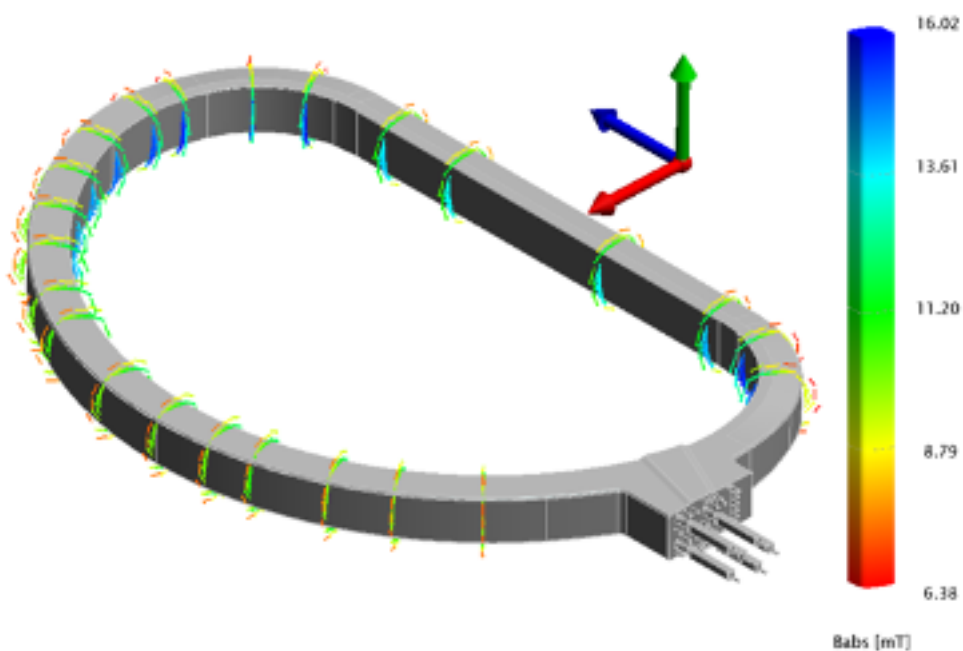


**Figure 12**. View of the entire WP magnetic flux density field at reduced current (200A) after numerical removal of the geomagnetic stray field. Vectors are proportional to the intensity |B| and are represented in the TGCS frame.
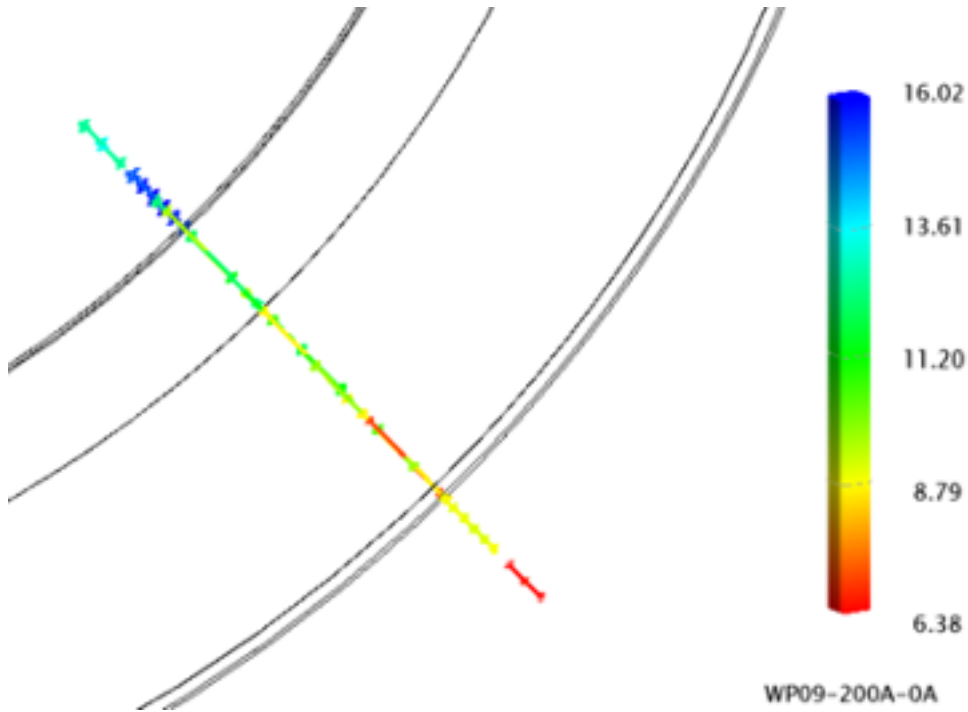
**Figure 13**. View of the magnetic field at reduced current (200A) after numerical removal of the stray field of a single section.
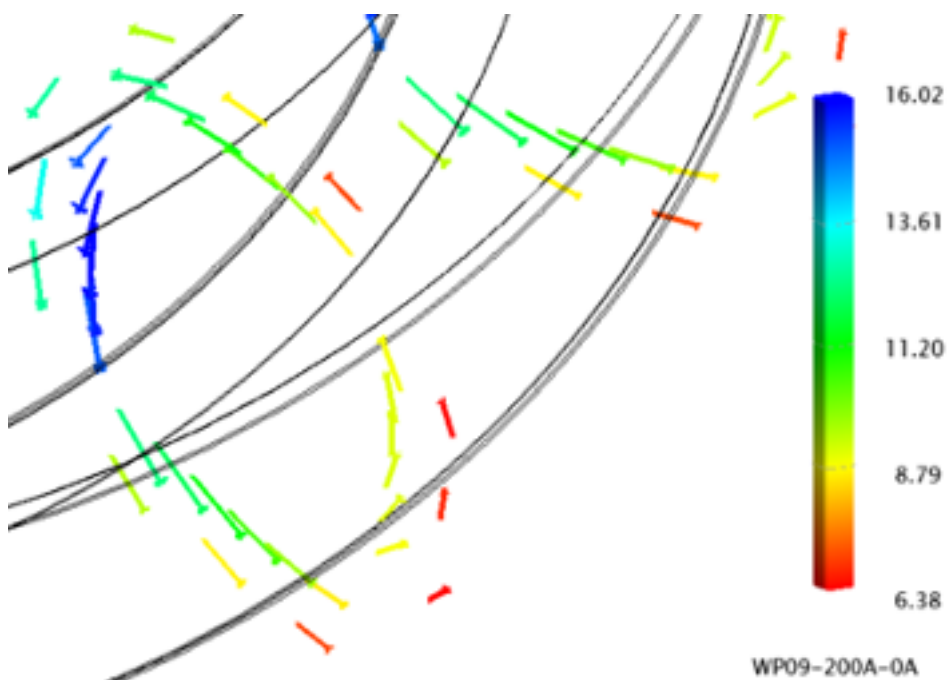


**Figure 14**. View of the magnetic field at reduced current (200A) after numerical removal of the stray field of the section in Figure 12.

## 4. Measurement statistics on 6 WPs

In the following pages, some statistic elements of the vector fields measured on 6 manufactured WPs are illustrated.

Definition: **Standard deviation σ** of the vector field of WPs at acquisition point "i"

$$\sigma_i = \sqrt{\frac{1}{N-1} \sum_{WP} \left( \vec{B}_{WPxi} - \left\langle \vec{B}_{WPxi} \right\rangle_{WP} \right)^2} \cdot 100\% \qquad \text{for } WP = 1, .., 6$$

Definition: **Magnetic Field Relative Difference** between WPx and average vector field of WPs at acquisition point "i"

$$\frac{dB_{WPi}}{B} = \frac{\| \vec{B}_{WPx} - \langle \vec{B}_{WPx} \rangle_i \|}{\| \langle \vec{B}_{WPx} \rangle_i \|} \cdot 100\%$$

Definition: **Geometrical Mean Deviation from Average**

$$\langle ds \rangle_{WP} = \left\| \left\langle \vec{dr}_{WPx} - \langle \vec{dr}_{WPx} \rangle_{WP} \right\rangle_i \right\|$$
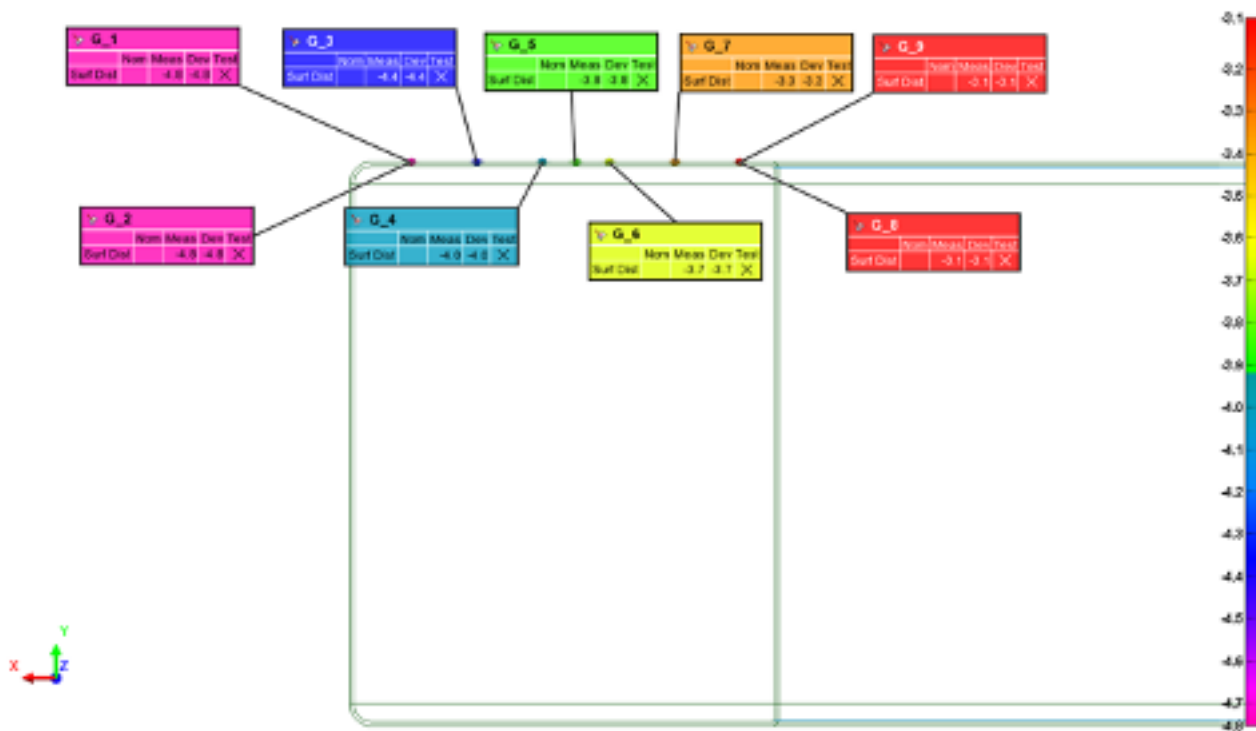


**Figure 15**. Deviation of the measured geometric surface from the nominal in correspondence to the projection of the measured magnetic points on the WP.
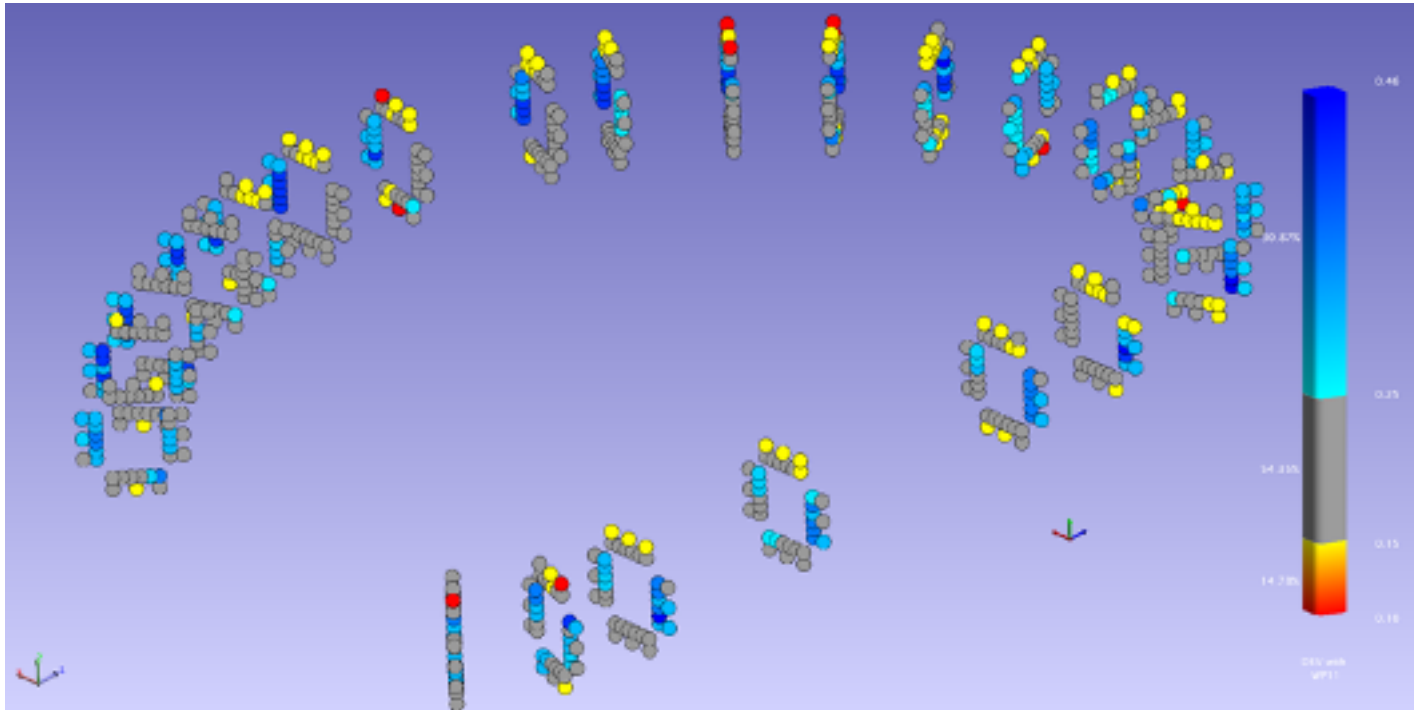
**Figure 16**. Standard deviation σ of 6 vector field of 6 different WPs [mT].
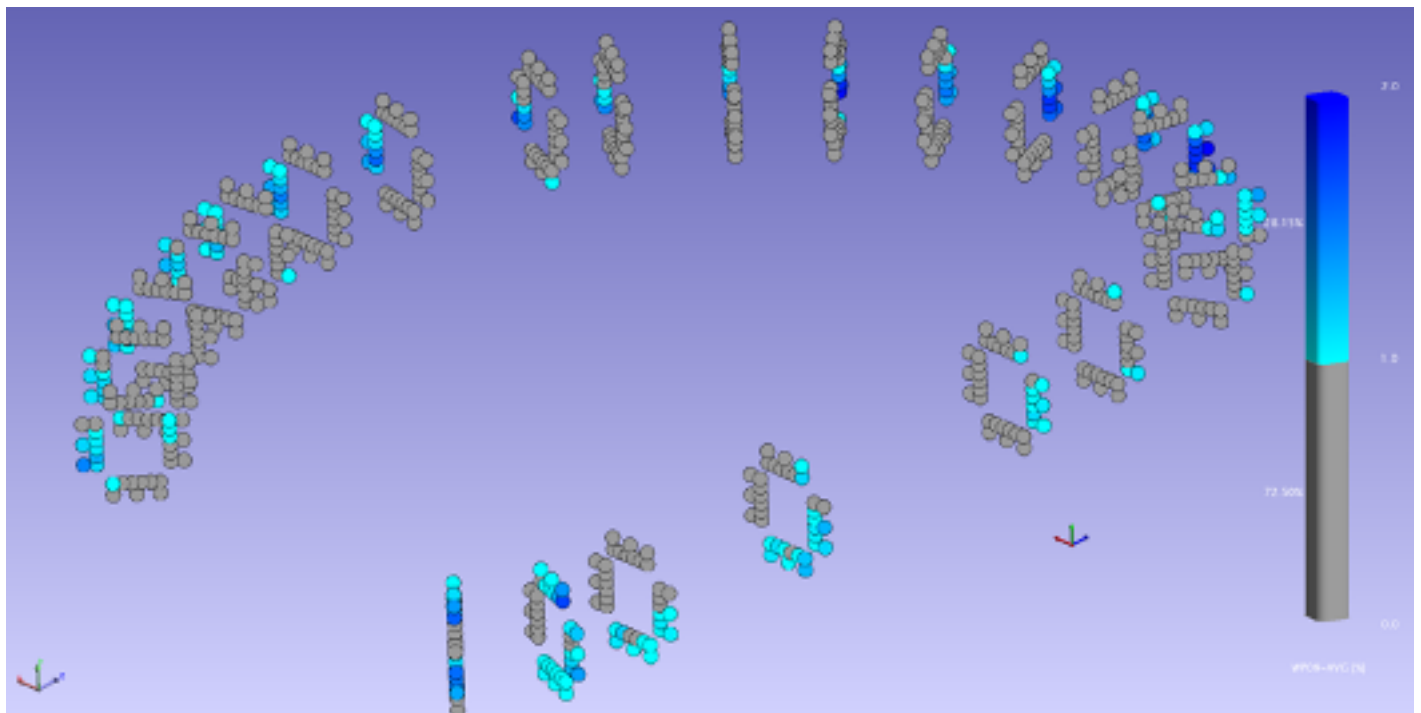


**Figure 17**. Relative difference $dB/B$ between WP09 and average.

In Figure 18 it is possible to appreciate the consistency of the geometrical manufacturing (horizontal axis) with respect to the consistency of the resulting magnetic field at reduced current (vertical axis).

Consistency of manufacturing is crucial to maximize the quality of the magnetic field generated by the Tokamak[6]. The more similar the WPs the higher the quality of the field.

[6] N. Mitchell and J. Knaster: "Contribution to Plasma Error Fields from the CS, PF and TF coils", ITER_D_23DVQU, v. 1.3: 2 September 2006.
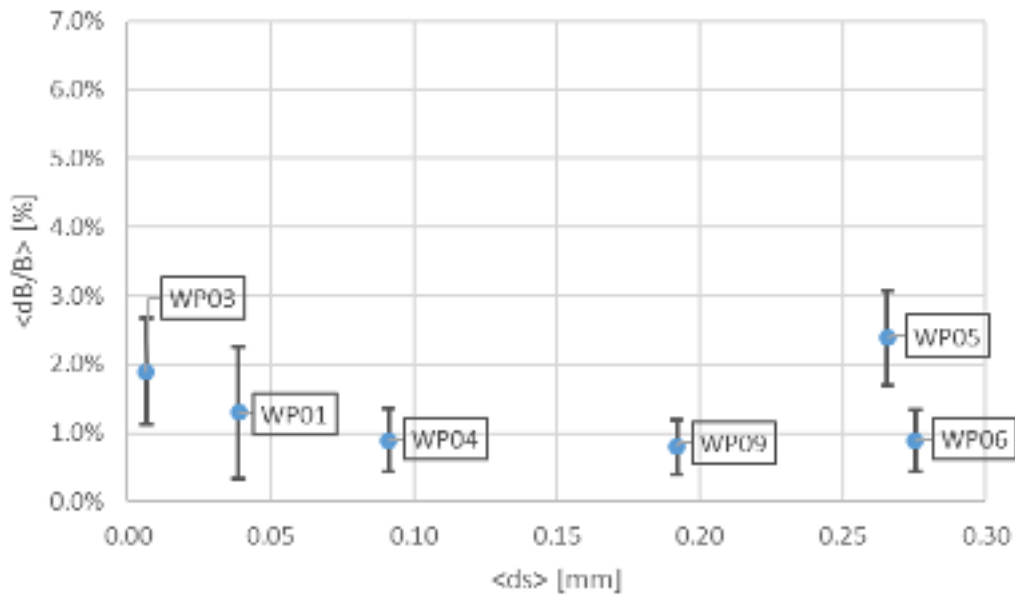
**Figure 18.** "Average Magnetic Field Relative Difference" <dB/B> plotted against the Geometrical Mean Deviation from Average $\langle ds \rangle$. Black error bars shows the standard deviation of the "Magnetic Field Relative Difference per each WP"